Theoretical Studies of the Substitution Patterns of Boron−Nitrogen (BN) Fullerenes: From C_{50} up to $C_{20}B_{15}N_{15}$ CBN Ball

Xiufang Xu,* Zhenfeng Shang, Guichang Wang, Ruifang Li, Zunsheng Cai, and Xuezhuang Zhao

Department of Chemistry, Nankai University, Tianjin, 300071, P. R. China

Received: January 14, 2005; In Final Form: March 4, 2005

Study on the patterns of successive BN pair substitution in C_{50} fullerene and the chemical and electronic properties of these substitutionally doped heterofullerenes has been carried out with semiempirical (AM1 and MNDO) and density functional (B3LYP/3-21G) theories. The BN units prefer to stay together following "single bond", "hexagon filling", and "continuity and equatorial belt" rules. The driving force governing the stabilities of these BN-doped fullerenes is the strain of the cage. Compared with C_{50}, the redox activity of $C_{50-2x}(BN)_x$ ($x = 1-15$) isomers decreases and becomes weaker by increasing the number of BN units, while the aromaticity of the $C_{50-2x}(BN)_x$ derivatives decreases and is independent of the number of BN units but related to the substitution positions. The main infrared absorptions are similar for all the $C_{50-2x}(BN)_x$ isomers and the infrared spectrum becomes simpler and stronger with increasing the number of BN groups.

Introduction

Heterofullerenes which have one or more carbon atoms substituted by other elements such as boron or nitrogen have been the subject of numerous experimental[1−5] and theoretical[6−19] studies because of their remarkable structural, electronic, optical, and magnetic properties. The first sign of substituted fullerenes $C_{60-x}B_x$ ($x = 1-6$) was detected by Smalley's group[1] in 1991. Later an avalanche of experimental studies on boron- or nitrogen-doped carbon clusters were reported, for instance, the nitrogen-doped C_{60} fullerene $C_{59}N$ was verified by Mattay et al.[2] and its dimmer $(C_{59}N)_2$ was isolated by Hummelen et al.[3] in 1995. Higher azafullerenes ($C_{60-2x}N_{2x}$, where $x = 1-23$) were synthesized by Glenis et al.[4] in 1994 and macroscopic quantities of B-doped fullerenes, such as $C_{60-x}B_x$ and $C_{70-x}B_x$ ($x = 1, 2$), were successfully synthesized by Cao et al.[5] in 1998.

Several theoretical investigations on heterofullerenes, namely $C_{59}B$,[6−9] $C_{58}B_2$,[10−14] $C_{60-x}B_x$ ($x = 2-8$),[15] and $C_{59}N$,[7−9,16] $C_{58}N_2$,[10−14] $C_{60-x}N_x$ ($x = 2-8$),[15] as well as smaller heterofullerenes, such as $C_{34}X_2$ (X = B, N),[17] $C_{38}X_2$ (X = B, N),[18] and $C_{48}X_2$ (X = B, N),[19] have been performed to understand the effect of B and N substitution on structure, and electronic and chemical properties of fullerenes.

Out of the heterofullerenes studied so far, overwhelming attention has been paid to the hybrid B/C/N fullerenes (or CBN ball). Synthesis of BN-substituted fullerenes has been reported: by an electric arc burning technique using a graphite anode having a hole filled with boron nitride in inert atmosphere,[20] by high-temperature laser ablation of graphite-like BCN,[21] by electron-beam irradiation of various precursors,[22,23] and by substitution reaction upon irradiation with a KrF excimer laser at room temperature.[24]

Several theoretical investigations[10,25−30] on mono-BN doped fullerenes have been reported. These studies indicate that heteroatoms prefer to stay together. Our group has extended the study of BN-substituted fullerenes by considering $C_{60-2x}(BN)_x$[31] and $C_{70-2x}(BN)_x$[32] ($x = 1-3$), using semiempirical AM1 and NMDO methods to predict their structure, stability, and electronic properties. Kar and co-workers have performed theoretical investigations[33,34] to study the structural patterns of successive substitution of 1−24 carbon pairs of C_{60} by BN moieties, and have established certain rules of successive BN substitution in fullerenes, such as "hexagonal filling rule" and "N-site rule". Their results also showed that not only the number of heteroatoms may tune the properties of BN-fullerenes but also their filling patterns.

The synthesis of low-mass fullerenes C_n ($n < 60$) on a macroscopic scale is an active field of current investigation. For example, the first preparation of C_{36} was claimed[35] in 1998, and the successful synthesis of the smallest possible fullerene C_{20} was reported[36] in 2000. As an important member of the fullerene family, C_{50} has long been considered to be the best preparation prospect for fullerenes smaller than C_{60}.[37,38] Fortunately, the first C_{50} derivative, decachlorofullerene[50] ($C_{50}Cl_{10}$), has been successfully prepared by Xie et al.[39] very recently, and the reason C_{50} itself, although it is a stable molecule, was not obtained experimentally is also suggested by them with density functional study: The equatorial pentagon−pentagon fusions of D_{5h} C_{50} are active sites for chemical reactions.[40] Our previous investigation[19] of heterofullerenes $C_{48}X_2$ (X = B, N) showed that the driving force governing the stabilities of the $C_{48}X_2$ (X = B, N) isomers is the strain being inherent in the C_{50} cage, especially the high strain of the equatorial belt of C_{50}. In this work, semiempirical AM1and MNDO and density functional theory (B3LYP/3-21G) investigation of the isomers of successive BN-substituted fullerenes $C_{50-2x}(BN)_x$ ($x = 1-15$) have been performed to examine the preferred substitution patterns, the relative stability, the electronic and chemical properties of these isomers, as well as the effect of successive substitution on those properties.

Method of Calculations

Investigations[17−19,31−34,41,42] of heterofullerenes have shown that although the quantitative aspects of relative energies are

* Corresponding author. E-mail: xxfang@nankai.edu.cn. Fax: +86-22-23502458. Phone: +86-22-23505244.

10.1021/jp050252s CCC: $30.25
Published on Web 04/02/2005

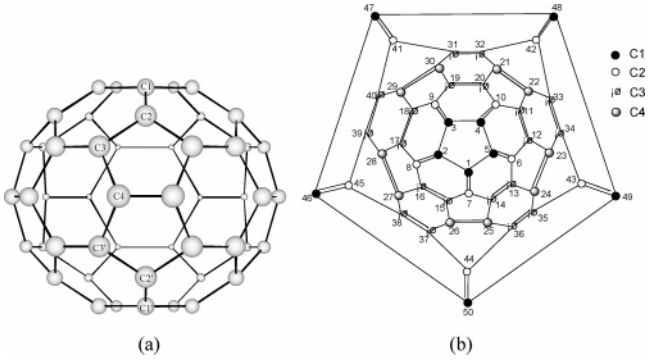

Figure 1. (a) Side view and (b) the Schlegel diagram of C_{50} (D_{5h}) showing the numbering system to discuss the $C_{50-2x}(BN)_x$ ($x = 1-15$) isomers.

sensitive to different methods (namely, AM1, MNDO, B3LYP/3-21G//MNDO, B3LYP/3-21G, PW91PW91/3-21G, etc.), the trend of relative energy is the same among all the methods, and the semiempirical AM1 and MNDO methods are quite reliable for determining the trends in relative stability and electronic properties. Therefore, full geometry optimizations were performed without any symmetry constraints in Cartesian coordinates at AM1 and MNDO levels for all possible isomers of BN-substituted fullerenes $C_{50-2x}(BN)_x$ ($x = 1-15$). Vibrational analysis at the AM1 and MNDO levels indicates that all the optimized isomers considered in the present investigation have no imaginary frequencies, suggesting the true minima. The geometries of some of the representative isomers are further optimized by using the B3LYP/3-21G method. For the most stable isomer of each group, the Gauge-Including Atomic Orbital (GIAO) NMR[43] calculations were carried out at the Hartree−Fock level with the 6-31G basis set to obtain the NICSs (nucleus independent chemical shifts), which has been used as a reliable criterion of aromaticity since it was proposed by Schleyer et al.[44] in 1996. Calculations of geometry optimizations, vibrational frequencies, and NMR were carried out with the Gaussian 98 program.[45]

Results and Discussion

A. Substitution Sequences of BN Groups. We have chosen the C_{50} cage with D_{5h} symmetry, which is fully optimized at the B3LYP/6-31G* level, as the parent molecule for doping, whose Schlegel diagram has been used in the present investigation. In this diagram (Figure 1) the 50 carbon atoms are numbered, and the categorized types of atoms and double bonds are also shown. It can be seen that there are six distinct kinds of CC bonds in C_{50}: C1−C1, C1═C2, C2−C3, C3═C3, C3−C4, and C4═C4. By replacing a carbon pair of the C_{50} cage with a BN group, and considering the different kinds of carbon atoms at each carbon pair, we obtain a total of 9 different $C_{48}BN$ isomers (Table 1). For the sake of convenience, a $C_{48}BN$ isomer is designated as BN:*i*−*j*, indicating that the carbon atoms with coding numbers of i and j are replaced by the B and N atoms, respectively. For example, BN:1−2 represents the $C_{48}BN$ isomer in which the carbon atoms with coding numbers 1 and 2 in the parent C_{50} cage are replaced by the B and N atoms, respectively. The AM1 and MNDO calculated heats of formation as well as the B3LYP/3-21G calculated electronic energies of all the $C_{48}BN$ isomers are listed in Table 1. We can see the following from Table 1: (i) The relative stability of the isomers is basically consistent at AM1, MNDO, and B3LYP/3-21G levels. Thermodynamically, BN:7−1 and BN:11−22 are the most stable isomers among them. It is worthwhile to note that

TABLE 1: AM1 and MNDO Heats of Formation (au) and B3LYP/3-21G Total Electronic Energies as Well as HF/6-31G//AM1 NICS for All Possible $C_{48}BN$ Isomers

substitution (B,N)	position	heat of formation AM1	heat of formation MNDO	B3LYP/3-21G	NICS
(1,2)	C1−C1	1.6365	1.4293	−1897.8046	−8.1
(1,7)	C1−C2	1.6218	1.4134	−1897.8291	−8.8
(7,1)		1.5646	1.3688	−1897.8308	
(6,13)	C2−C3	1.5838	1.4284	−1897.8137	−10.6
(13,6)		1.5980	1.4274	−1897.8038	
(11,12)	C3−C3	1.6112	1.4046	−1897.8157	−26.4
(11,22)	C3−C4	1.5652	1.3607	−1897.8314	−12.0
(22,11)		1.5674	1.3760	−1897.8185	
(21,22)	C4−C4	1.5906	1.3866	−1897.8281	−27.9

TABLE 2: AM1 and MNDO Heats of Formation (au) for All Possible $C_{46}(BN)_2$ Isomers

substitution position (B,N,B,N)	heat of formation AM1	heat of formation MNDO
(11,22,23,12)	1.5165	1.2709
(11,22,4,10)	1.5273	1.2732
(11,22,21,32)	1.5292	1.2816
(11,22,21,20)	1.5303	1.2850
(11,22,33,34)	1.5360	1.2843
(11,22,6,12)	1.5469	1.2986
(11,22,33,42)	1.5515	1.2978
(11,22,20,10)	1.5560	1.3017

the doping position in the former is the C1═C2 double bond, and in the latter it is the C3−C4 single bond, which is different from the single-BN doping in C_{40}[18] and C_{60}[31] where the only preferred substitution position is the C═C double bond. (ii) For BN-substitution taking place at the carbon pairs near the poles of the carbon cage, the more stable product is the one in which the carbon atom with less strain is substituted by the N atom, for example, BN:7−1 is more stable than BN:1−7. However, as the BN group replaces the carbon pairs near the equator of the carbon cage, the more stable product generated is the one in which the carbon atom with greater strain is substituted by the N atom, for instance, BN:11−22 is more stable than BN:22−11. On the whole, the nearer the BN group is to the equator, the more stable the isomer is. According to the conclusions obtained in our previous research of $C_{48}X_2$ (X = B, N),[19] we suggest that the driving force governing the stabilities of the BN-doped fullerenes under this investigation is also the strain of the cage, which is also reflected in the bond length increment in [5,5] bonds after doping (data are not shown here).

BN substitution will release some strain of the carbon cage, and the more the strain is released, the more stable the heterofullerene is. In general, the isomer with the BN unit closer to the equator is more stable, since the nearer the carbon bond of the C_{50} cage is to the equator the greater the strain of the carbon bond. Thus, we choose the isomer BN:11−22 as the parent cage to continue replacing CC pairs. It is expected that the new incoming BN units spreading around the 11−22 position will release more strain than those spreading around the 7−1 position. According to the B−N junction rule,[31−34] we construct 8 distinct 2-BN isomers of $C_{46}(BN)_2$ whose heats of formation are listed in Table 2. We can see from Table 2 that the most favored substitution position for the second incoming BN unit is the 23−12 CC pair, which is closely followed by 4−10 and 21−32 positions. Inspection of the substitution positions and the stabilities of the isomers in Table 2 shows the following: (i) The second BN unit still prefers to replace the C3−C4 carbon pair and connect to the first BN group with the B-site to form an attachment of B−NB, which is different from the N-site attachment rule concluded by Pattanayak et al.[33]

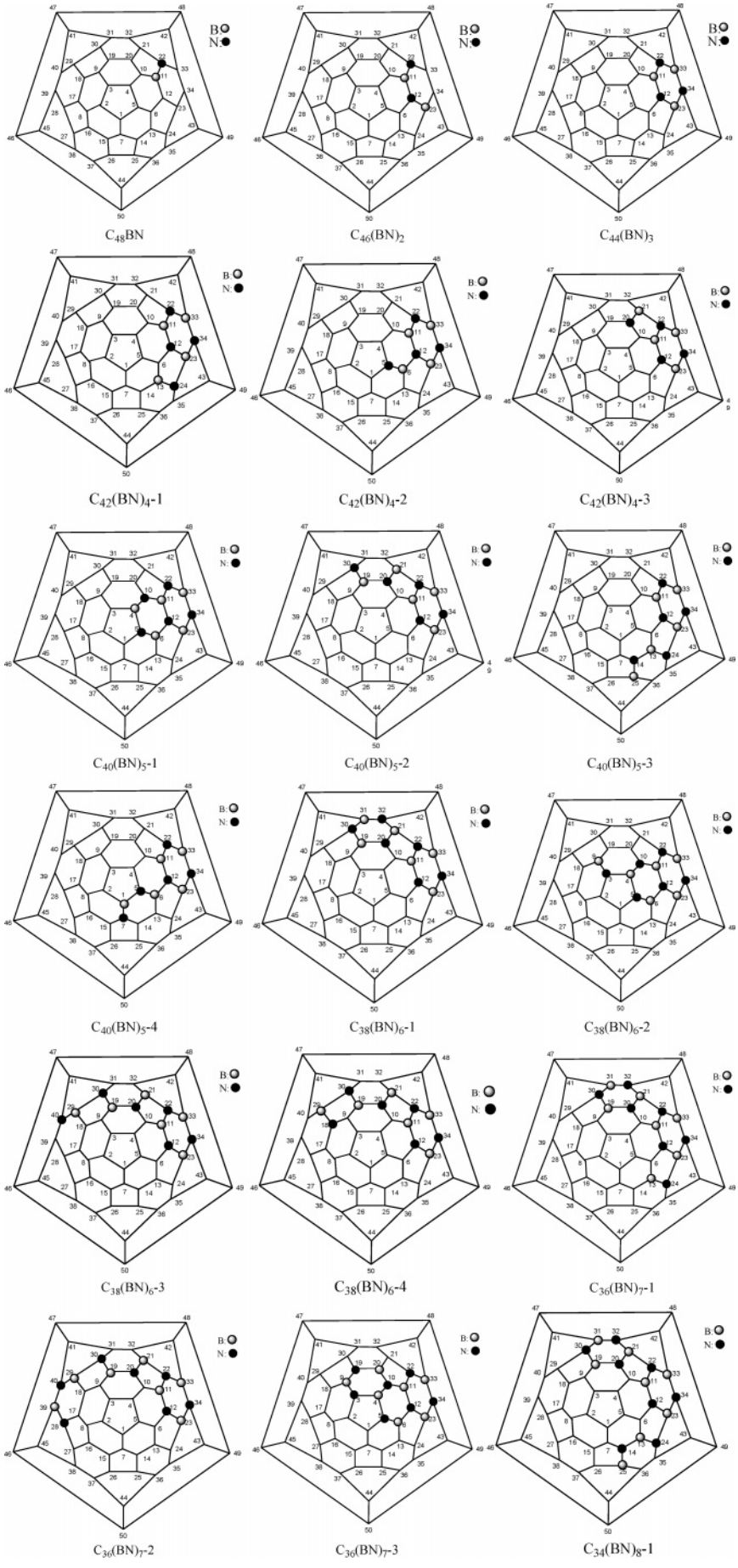
B
N
$C_{48}BN$
$C_{46}(BN)_2$
$C_{44}(BN)_3$
$C_{42}(BN)_4$-1
$C_{42}(BN)_4$-2
$C_{42}(BN)_4$-3
$C_{40}(BN)_5$-1
$C_{40}(BN)_5$-2
$C_{40}(BN)_5$-3
$C_{40}(BN)_5$-4
$C_{38}(BN)_6$-1
$C_{38}(BN)_6$-2
$C_{38}(BN)_6$-3
$C_{38}(BN)_6$-4
$C_{36}(BN)_7$-1
$C_{36}(BN)_7$-2
$C_{36}(BN)_7$-3
$C_{34}(BN)_8$-1

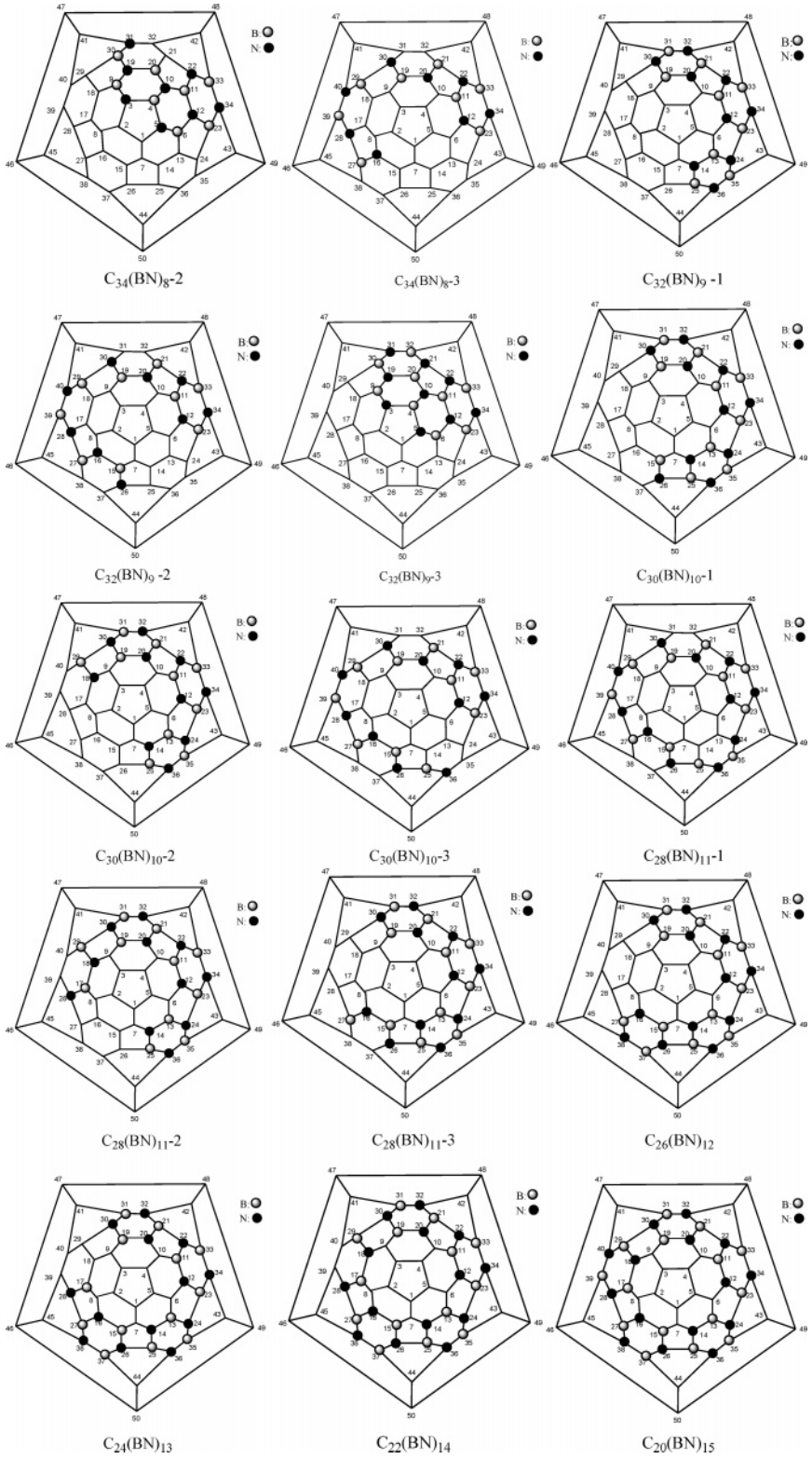

Figure 2. The 1-BN to 15-BN substitution patterns.

in their study of BN-dope C_{60} fullerenes. (ii) Isomers in which two BN units locate at the same side of the equator or at two abutting hexagons are more stable than those in which two BN units lie at the different sides of the equator. According to the "as many B−N bonds as possible" rule[33,34] and "hexagon-filling" rule (see Conclusion), the third BN unit is expected to prefer to replace the 33−34 carbon pair of the favored 2-BN isomer, and the calculated results confirm this. The favored substitution patterns of the 1-BN to 3-BN isomers are shown in Figure 2.

We proceed to further replace 1−12 carbon pairs from 3-BN fullerene to finally form $C_{20}B_{15}N_{15}$. The heats of formation for the thermodynamically most stable isomer of each replacing group at the AM1 and MNDO levels and the total electronic energies at the B3LYP/3-21G level are listed in Table 3. One can see from Table 3 that both the heat of formation and the total electronic energy of these isomers decrease with the increase of BN units. The substitution patterns for these stable isomers are summarized in Figure 2. In each group, we arrange the isomers in order of their stability, for example, the stability

TABLE 3: The AM1 and MNDO Heats of Formation (au) and B3LYP/3-2G Total Electronic Energies (au) of the Most Stable Isomer for Each Group

isomer	AM1	MNDO	B3LYP/3-21G	isomer	AM1	MNDO	B3LYP/3-21G
$C_{48}BN$-1	1.5652	1.3607	−1897.8313	$C_{32}(BN)_9$-1	1.1842	0.6025	−1925.6396
$C_{46}(BN)_2$	1.5165	1.2709	−1901.3007	$C_{30}(BN)_{10}$-1	1.1470	0.5084	−1929.0991
$C_{44}(BN)_3$	1.4685	1.1742	−1904.7881	$C_{28}(BN)_{11}$-1	1.0865	0.4018	−1932.5783
$C_{42}(BN)_4$-1	1.4318	1.0805	−1908.2543	$C_{26}(BN)_{12}$	1.0406	0.3153	−1936.0660
$C_{40}(BN)_5$-1	1.3687	0.9768	−1911.7544	$C_{24}(BN)_{13}$	1.0003	0.2186	−1939.5338
$C_{38}(BN)_6$-1	1.3270	0.8889	−1915.2138	$C_{22}(BN)_{14}$	0.9212	0.1003	−1943.0359
$C_{36}(BN)_7$-1	1.2900	0.7950	−1918.6799	$C_{20}(BN)_{15}$	0.8662	−0.0007	−1946.5240
$C_{34}(BN)_8$-1	1.2410	0.7053	−1922.1491				

order for the three favored 4-BN heterofullerene isomers is $C_{42}(BN)_4$-1 > $C_{42}(BN)_4$-2 > $C_{42}(BN)_4$-3. With inspection of these substitution patterns we can see the following: (i) When the BN units go up to 6, 9, 12, and 15, the most favored heterofullerenes are those in which 2, 3, 4, and 5 adjacent hexagons at the equator are filled with BN units, respectively. Interestingly, one can see that the most stable 11-BN isomer has a special structure: except for a full-filled hexagon by BN units, each of the rest of the hexagons at the equator is partially filled with two BN units and the BN units interlace at different sides of the equator. (ii) In the case of 1-BN to 10-BN substitutions, the incoming BN units can spread in two favorable directions: one is along the hexagons at the equator, the other is from the hexagons at the equator to the adjacent hexagons near the equator, while for the substitutions of more than 10 BN units, the favored positions for the incoming BN units are CC pairs of the hexagons at the equator. (iii) Depending on the number of substituted BN units and the location of the substitution position, the connection of the incoming BN unit will take place by attaching to either the N atom (called N-site attachment) or the B atom (called B-site attachment) of an existing BN group.

When the number of BN units goes up to 15, the six hexagons at the equator are fully filled, forming a close B−N belt. This is the most stable isomer, $C_{20}(BN)_{15}$, among the BN-doped heterofullerenes generated from C_{50} and is expected to be a potential CBN ball material. In Figure 3 the B3LYP/3-21G optimized geometry of $C_{20}(BN)_{15}$ is shown. It can be seen from Figure 3 that N atoms are moved outward and B atoms are displaced inward forming a wavelike surface along the equator belt. The population of Mulliken charge for $C_{20}(BN)_{15}$ is listed in Table 4. We note that because of the electronegativity differences, B and N atoms in $C_{20}(BN)_{15}$ bear positive and negative charge, respectively, and the B (or N) atoms at C4 positions bear more charge than those at C3 positions, while the carbon atoms are nearly electrically neutral.

B. Aromaticity. Aromaticity is commonly explained by the ring current theory[46,47] that attributes the unique properties shared by aromatic molecules to form a special electron delocalization, that is, the geometry of the conjugate molecule

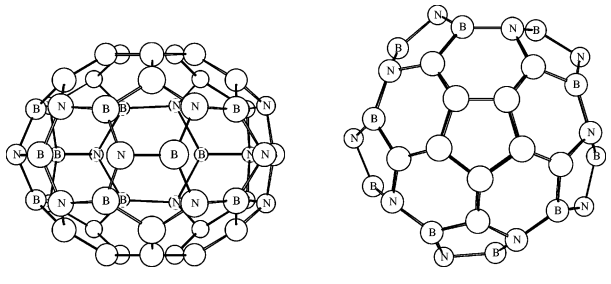

Figure 3. B3LYP/3-21G optimized geometry of $C_{20}(BN)_{15}$: (a) viewing perpendicular to the principal axis and (b) viewing along the principal axis.

TABLE 4: B3LYP/3-21G Calculated Mulliken Charge for $C_{20}(BN)_{15}$

atom type	Mulliken charge
C1	−0.0438
C2	−0.1164
B(C3)	0.8522
N(C3)	−0.7333
B(C4)	0.8875
N(C4)	−0.8046

TABLE 5: HF/6-31G//AM1 Calculated NICS for $C_{50-2x}(BN)_x$ ($x = 1-15$) Isomers

isomer	NICS	isomer	NICS	isomer	NICS
$C_{48}BN$-1	−12.0	$C_{38}(BN)_6$-1	−14.1	$C_{28}(BN)_{11}$-1	−13.9
$C_{46}(BN)_2$	−15.0	$C_{36}(BN)_7$-1	−14.2	$C_{26}(BN)_{12}$	−12.7
$C_{44}(BN)_3$	−14.2	$C_{34}(BN)_8$-1	−14.4	$C_{24}(BN)_{13}$	−11.7
$C_{42}(BN)_4$-1	−14.4	$C_{32}(BN)_9$-1	−13.6	$C_{22}(BN)_{14}$	−11.5
$C_{40}(BN)_5$-1	−13.3	$C_{30}(BN)_{10}$-1	−13.5	$C_{20}(BN)_{15}$	−10.7

allows the electrons to move along a cyclic path for delocalization, and the aromaticity of the doped isomer is affected by the doping position. The degree of electron delocalization is evaluated by using the computed NICS (nucleus independent chemical shifts),[44] which been demonstrated to be a useful criterion for aromaticity or antiaromaticity.[48,49] The calculated NICSs for the most stable isomers of 1-BN to 15-BN heterofullerenes of C_{50} are listed in Table 5. According to the definition of NICS, the more negative the value of NICS the more aromatic the molecule. Compared with the endohedral chemical shift of C_{50}, −28.8 ppm, the aromaticity of the BN-doped isomers, with NICSs between −10.7 and −15.0 ppm, decreases in general. On the other hand, it seems that NICSs of these isomers are independent of the number of substituted BN units. In fact, in each of the isomers listed in Table 5 at least one C3−C4 carbon pair is replaced by a BN group, and once substitution takes place at the C3−C4 position, the equatorial [5,5] double bonds, which connect the two spheres of the C_{50} cage to become a big conjugate system, will be elongated to single bonds. For example, in C_{50} the [5,5] double bond is 1.397 Å, after single-BN substitution, the longest [5,5] bond in the most stable $C_{48}BN$ isomer is 1.491 Å at the MNDO level. Consequently, the conjugate structure of the parent C_{50} cage is destroyed greatly, and the degree of electron delocalization decreases. We note in passing, the NICS value of the heterofullerene should be doping-site dependent (Table 1).

C. HOMO-LUMO Gap, Ionization Potentials, and Electron Affinities. In our previous investigation[19] we found that the substitutional perturbation affects both the HOMO and LUMO for $C_{48}X_2$ (X = B, N). Roughly speaking, the HOMO energies become higher while the LUMO energies become lower with increasing heats of formation, and the HOMO-LUMO energy gaps decrease with increasing heats of formation.

According to Koopmans' theorem, IP = $-E_{HOMO}$, EA = $-E_{LUMO}$. The ionization potentials ($-E_{HOMO}$), electron affinities ($-E_{LUMO}$), and HOMO-LUMO energy gaps for $C_{50-2x}(BN)_x$ (x

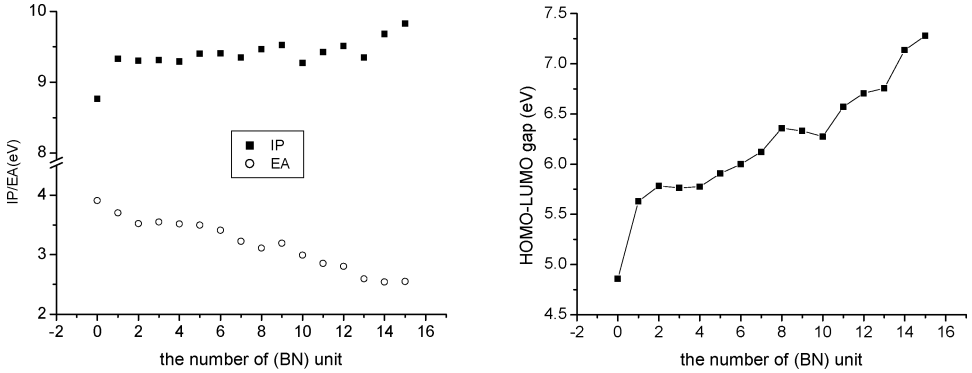

Figure 4. Dependence of IP, EA, and HOMO-LUMO gap on the number of (BN) units based on the AM1 calculated results.

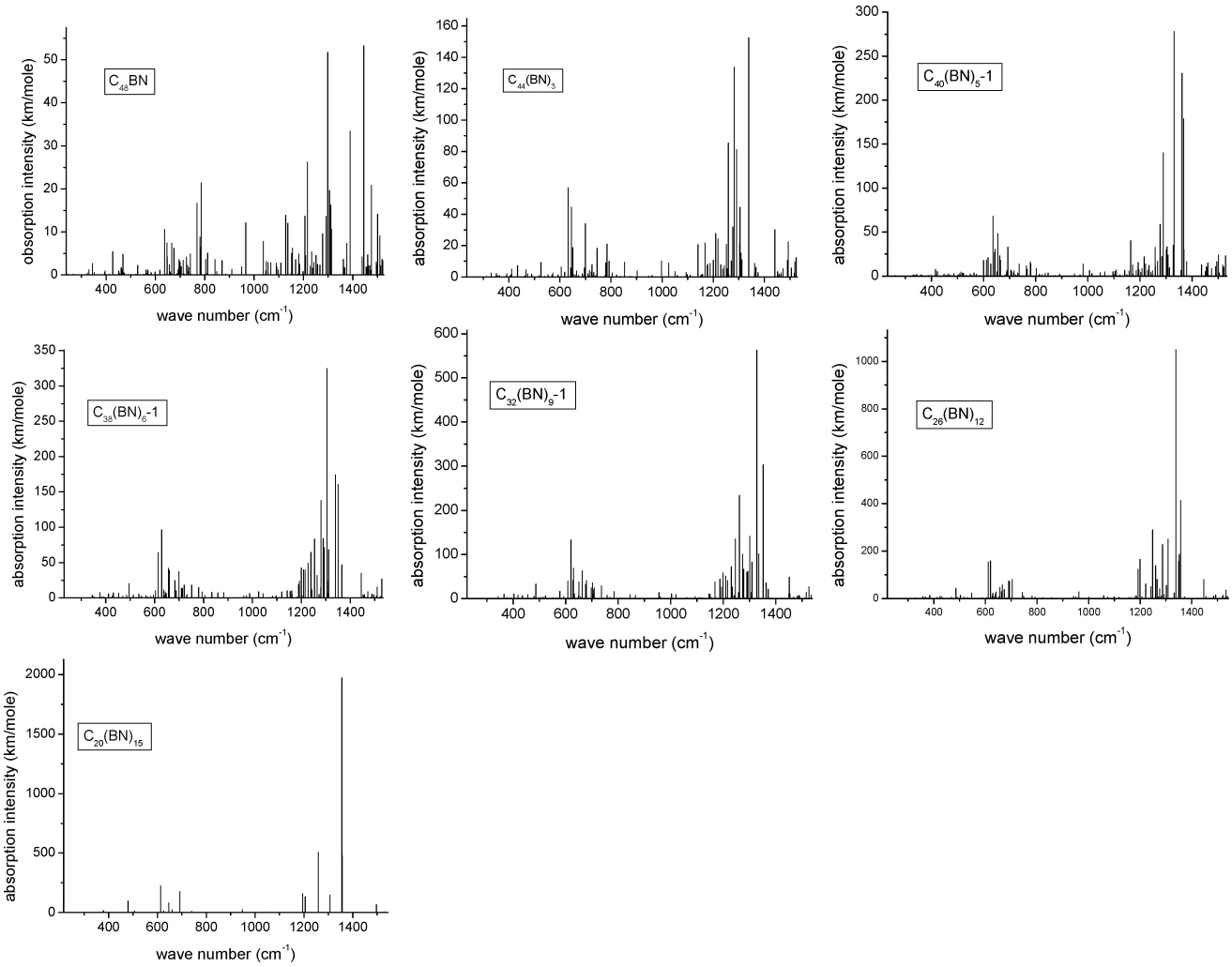

Figure 5. MNDO calculated vibrational spectra of $C_{50-2x}(BN)_x$ (x = 1, 3, 5, 6, 9, 12, 15).

= 1−15) are summarized in Figure 4. In general, the IP becomes higher while the EA becomes lower with increasing the number (x) of BN units, which is somewhat different from that of the BN-doping in C_{40}[18] and C_{60}.[31] Figure 4 also indicates that the $C_{50-2x}(BN)_x$ isomers have bigger ionization potentials ($-E_{HOMO}$) and smaller electron affinities ($-E_{LUMO}$) compared with C_{50}, which suggests that the $C_{50-2x}(BN)_x$ isomers not only lose electrons with somewhat more difficulty to form positive ions but also obtain electrons with more difficulty to form anions, i.e., it is more difficult to oxidize or reduce $C_{50-2x}(BN)_x$ than C_{50}. Moreover, the redox activity becomes weaker with increasing the number (x) of BN units.

The HOMO-LUMO energy gaps are associated with the chemical stabilities against electronic excitation. There is a general trend that the HOMO-LUMO energy gaps increase with increasing the number (x) of BN units, and the gaps of the $C_{50-2x}(BN)_x$ isomers are larger than that of C_{50}, suggesting an electron in $C_{50-2x}(BN)_x$ is more difficult to excite from the HOMO to the LUMO in those isomers than in C_{50}, the bigger the x is, the more difficult it is to excite an electron in this heterofullerene. For example, the HOMO-LUMO energy gap for C_{50} is 4.86 eV, while that for $C_{20}(BN)_{15}$ is up to 7.28 eV.

D. Vibrational Spectrum. The MNDO calculated infrared spectra of several representative $C_{50-2x}(BN)_x$ isomers are shown

in Figure 5. The calculated frequencies have been scaled down uniformly by a factor of 0.89.[50,51] We can see from Figure 5 that the frequencies of the main infrared absorptions are similar for all the $C_{50-2x}(BN)_x$ isomers: The stronger absorptions at 1200−1400 cm^{-1} derive from the stretching of C−B, C−N, B−N, and C═C bonds, while the weaker absorptions at 600−800 cm^{-1} correspond to the bond bending of C−C and the cage skeleton. On the other hand, one can see from Figure 5 that the vibrational spectrum becomes simpler and the intensity of the vibrational absorptions at 1200−1400 cm^{-1} increases with increasing the number of BN groups, and the 15-BN isomer has the simplest spectrum and the greatest intensity of vibrational absorptions at 1200−1400 cm^{-1} than other isomers.

Conclusion

To establish the pattern of successive substitution of carbon pairs of C_{50} fullerene by isoelectronic BN moieties, a large number of BN-substituted fullerenes have been considered, using semiempirical and density functional theories. Although numerical values differ, for example, the heats of formation calculated at the AM1 level are about 0.19−0.87 au higher than those calculated at the MNDO level for the $C_{50-2x}(BN)_x$ isomers, the trends in structure, stability, and electronic properties are consistent at different theoretical levels. The HOMO-LUMO energy gaps, ionization potentials, electronic affinities, and vibrational spectra of the $C_{50-2x}(BN)_x$ isomers have also been studied at the AM1 and MNDO levels, and the NICSs which represent the aromaticity of the isomers have been studied by using the HF/6-31G method at AM1 optimized geometries.

From the results obtained in the present investigation we emphasize the following important points on the successive substitution pattern:

(i) Single Bond Rule: The driving force governing the stabilities of the heterofullerenes[50] is the strain inherent in the C_{50} cage. Substitution of the C3−C4 carbon pair by a BN group will elongate all the [5,5] double bonds at the equator, consequently, the high strain of the equator is released and the generated heterofullerenes are stabilized. This is different from the BN-substitution in C_{40} and C_{60} where the preferred substitution position is the C═C double bond.

(ii) Hexagon-Filling Rule: BN units prefer to fill available sites in consecutive hexagons. This pattern increases the number of B−N bonds. Thus, once the first substitution takes place, the next two BN units replace the carbons of the same hexagon.

(iii) Continuity Rule and Equatorial Belt Rule: Joining existing BN units to spread over different hexagons significantly enhances the stability. In the case of 1-BN to 10-BN substitutions, the incoming BN units can spread in two favorable directions: one is along the hexagons at the equator, the other is from the hexagons at the equator spreading to the adjacent hexagons near the equator, while for the substitutions of more than 10 BN units, the favored positions for the incoming BN units are CC pairs of the hexagons at the equator.

In addition, our results also show that the stability and the electronic and chemical properties of these hemterofullerences can be tuned by the number of BN units and the substitution patterns, which includes the following general features:

(i) Compared with C_{50}, the aromaticity of the $C_{50-2x}(BN)_x$ derivatives decreases and is independent of the number of BN units but related to the substitution positions.

(ii) Compared with C_{50}, the redox activity of $C_{50-2x}(BN)_x$ isomers decreases and becomes weaker with an increasing number of BN units. This is different from that of the BN-doped C_{40} and C_{60} heterofullerenes: when BN units are less than a certain proportion, the redox activity of the heterofullerenes is stronger than that of the parent carbon cage, while when they are more than the proportion, the redox activity is weaker than that of the parent carbon cage.

(iii) The main infrared absorptions are similar for all the $C_{50-2x}(BN)_x$ isomers and the infrared spectrum becomes simpler and stronger with an increasing number of BN groups.

(iv) $C_{20}(BN)_{15}$ is thermodynamically and chemically the most stable isomer and is expected to be a potential CBN ball material.

Acknowledgment. This work was supported by the National Nature Science Foundation of China under Project 20303010, the Science Foundation of Nankai University, and Nankai University ISC.

References and Notes

(1) Guo, T.; Jin, C.; Smally, R. E. *J. Chem. Phys.* **1991**, *95*, 4948.
(2) Averdung, J.; Luftmann, H.; Sch-achter, I.; Mattay, J. *Tetrahedron* **1995**, *51*, 6977.
(3) Pavlovich, J.; Gonzalez, R.; Hummelen, J. C.; Knight, B.; Wudl, F. *Science* **1995**, *269*, 1554.
(4) Glenis, S.; Cooke, S.; Chen, X.; Labes, M. M. *Chem. Mater*. **1994**, 6.
(5) Cao, B.; Zhou, X.; Shi, Z.; Gu, Z.; Xiao, H.; Wang, J. *Fullerene Sci. Technol.* **1998**, *6*, 639.
(6) Miyamoto, Y.; Hamada, N.; Oshiyama, A.; Saito, S. *Phys. Rev. B* **1992**, *46*, 1749.
(7) Andreoni, W.; Gygi, F.; Parrinello, M. *Chem. Phys. Lett.* **1992**, *190*, 159.
(8) Kurita, N.; Kobayashi, K.; Kumahora, H.; Tago, K.; Ozawa, K. *Chem. Phys. Lett.* **1992**, *198*, 95.
(9) Chen, F.; Singh, D.; Jansen, S. A. *J. Phys. Chem.* **1993**, *97*, 10958.
(10) Kurita, N.; Kobayashi, K.; Kumahora, H.; Tago, K. *Fullerene Sci. Technol*. **1993**, *1*, 319.
(11) Kurita, K.; Kobayashi, K.; Kumahora, H.; Tago, K. *Phys. Rev. B* **1993**, *48*, 4850.
(12) Wang, S. H.; Chen, F.; Fann, Y. C.; Kashani, M.; Malaty, M.; Jansen, S. A. *J. Phys. Chem.* **1995**, *99*, 6801.
(13) Chen, Z.; Ma, K.; Pan, Y.; Zhao, X.; Tang, A.; Feng, J. *J. Chem. Soc., Faraday Trans.* **1998**, *94*, 2269.
(14) Chen, Z.; Ma, K.; Pan, Y.; Zhao, X.; Tang, A. *Can. J. Chem*. **1999**, *77*, 291.
(15) Chen, Z.; Zhao, X.; Tang, A. *J. Phys. Chem. A* **1999**, *103*, 10961.
(16) Andreoni, W.; Curioni, A.; Holczer, K.; Prassides, K.; Keshavarz-K, M.; Hummelen, J.-C.; Wudl, F. *J. Am. Chem. Soc.* **1996**, *118*, 11335.
(17) Yang, Z.; Xu, X.; Wang, G..; Shang, Z.; Cai, Z.; Pan, Y.; Zhao, X. *J. Mol. Struct.* (*THEOCHEM*) **2002**, *618*, 191.
(18) Yang, X.; Wang, G.; Shang, Z.; Pan, Y.; Cai, Z.; Zhao, X. *Phys. Chem. Chem. Phys.* **2002**, *4*, 2546.
(19) Xu, X.; Xing, Y.; Shang, Z.; Wang, G.; Cai, Z.; Pan, Y.; Zhao, X. *Chem. Phys.* **2003**, *287*, 317.
(20) Piechota, J.; Byzsewski, P.; Jablonski, R.; Antonova, K. *Fullerene Sci. Technol.* **1996**, *4*, 491.
(21) Nakamura, T.; Ishikawa, K.; Yamamoto, K.; Ohana, T.; Fujiwara, S.; Koga, Y. *Phys. Chem. Chem. Phys.* **1999**, *1*, 2631.
(22) Golberg, D.; Bando, Y.; Stephan, O.; Kurashima, K.; Sasaki, T.; Sato, T.; Goringe, C. In *International Conference on Solid-State Phase Transformations* (*JIMIC-3*); Koiwa, M., Otsuka, K., Miyazaki, T., Eds.; Japan, 1999; pp 1301−1304.
(23) Golberg, D.; Bando, Y.; Stephan, O.; Bourgeois, L.; Kurashima, K.; Sasaki, T.; Sato, T.; Goringe, C. *J. Electron Microsc.* **1999**, *48*, 701.
(24) Nakamura, T.; Ishikawa, K.; Goto, A.; Ishihara, M.; Ohana, T.; Koga, Y. *Diamond Relat. Mater.* **2001**, *10*, 1228.
(25) Liu, J.; Gu, B.; Han, R. *Solid State Commun.* **1992**, *84*, 807.
(26) Esfarjani, K.; Ohno, K.; Kawazoe, Y. *Phys. Rev. B* **1994**, *50*, 17830.
(27) Esfarjani, K.; Ohno, K.; Kawazoe, Y. *Surf. Rev. Lett.* **1996**, *3*, 747.
(28) Esfarjani, K.; Ohno, K.; Kawazoe, Y.; Gu, B.-L. *Solid State Commun.* **1996**, *97*, 539.
(29) Piechota, J.; Byszewski, P. Z. *Phys. Chem.* **1997**, *200*, 147.
(30) Shkrabo, D. M.; Krasyukov, Y. N.; Mukhtarov, E. I.; Zhizhin, G. N. *J. Struct. Chem.* **1998**, *39*, 323.
(31) Chen, Z.; Ma, K.; Zhao, H.; Pan, Y.; Zhao, X.; Tang, A.; Feng, J. *J. Mol. Struct.* (*THEOCHEM*) **1999**, *466*, 127.
(32) Chen, Z.; Ma, K.; Pan, Y.; Zhao, X.; Tang, A. *J. Mol. Struct.* (*THEOCHEM*) **1999**, *490*, 61.
(33) Pattanayak, J.; Kar, T.; Scheiner, S. *J. Phys. Chem A* **2001**, *105*, 8376.

(34) Pattanayak, J.; Kar, T.; Scheiner, S. *J. Phys. Chem A* **2002**, *106*, 2970.

(35) Piskoti, C.; Yarger, J.; Zettl, A. *Nature* **1998**, *393*, 771.

(36) Prinzbach, H.; Weller, A.; Landenberger, P.; Wahl, F.; Worth, J.; Scott, L. T.; Gelmont, M.; Olevano, D.; von Issendorff, B. *Nature* **2000**, *407*, 60.

(37) Kroto, H. W. *Nature* **1987**, *329*, 529.

(38) Heath, J. R. *Nature* **1998**, *393*, 730.

(39) Xie, S. Y.; Gao, F.; Lu, X.; Huang, R. B.; Wang, C. R.; Zhang, X.; Liu, M. L.; Deng, S. L.; Zheng, L. S. *Science* **2004**, *304*, 699.

(40) Lu, X.; Chen, Z.; Thiel W.; Schleyer, P. v. R.; Huang, R.; Zheng, L. *J. Am. Chem. Soc*. **2004**, *126*, 14871.

(41) Kar, T.; Pattanayak, J.; Scheiner, S. *J. Phys. Chem A* **2003**, *107*, 8630.

(42) Pattanayak, J.; Kar, T.; Scheiner, S. *J. Phys. Chem A* **2004**, *108*, 7681.

(43) Wolinski, K.; Hilton, J. F.; Pulay, P. *J. Am. Chem. Soc*. **1990**, *112*, 8251.

(44) Schleyer, P. v. R.; Maerker, C.; Dransfeld, A.; Jiao, H.; Hommes, N. J. R. v. E. *J. Am. Chem. Soc.* **1996**, *118*, 6317.

(45) Frisch, M. J.; Trucks, G. W.; Schlegel, H. B.; Scuseria, G. E.; Robb, M. A.; Cheeseman, J. R.; Zakrzewski, V. G.; Montgomery, J. A., Jr.; Stratmann, R. E.; Burant, J. C.; Dapprich, S.; Millam, J. M.; Daniels, A. D.; Kudin, K. N.; Strain, M. C.; Farkas, O.; Tomasi, J.; Barone, V.; Cossi, M.; Cammi, R.; Mennucci, B.; Pomelli, C.; Adamo, C.; Clifford, S.; Ochterski, J.; Petersson, G. A.; Ayala, P. Y.; Cui, Q.; Morokuma, K.; Malick, D. K.; Rabuck, A. D.; Raghavachari, K.; Foresman, J. B.; Cioslowski, J.; Ortiz, J. V.; Stefanov, B. B.; Liu, G.; Liashenko, A.; Piskorz, P.; Komaromi, I.; Gomperts, R.; Martin, R. L.; Fox, D. J.; Keith, T.; Al-Laham, M. A.; Peng, C. Y.; Nanayakkara, A.; Gonzalez, C.; Challacombe, M.; Gill, P. M. W.; Johnson, B. G.; Chen, W.; Wong, M. W.; Andres, J. L.; Head-Gordon, M.; Replogle, E. S.; Pople, J. A. *Gaussian 98*, revision A.7; Gaussian, Inc.: Pittsburgh, PA, 1998.

(46) Pauling, L. *J. Chem. Phys.* **1936**, *4*, 673.

(47) Lonsdale, K. *Proc. R. Soc. London, Ser. A* **1937**, *159*, 149.

(48) Schleyer, P. v. R.; Jiao, H.; Hommes, N. J. R. v. E.; Malkin, V. G.; Malkin, O. *J. Am. Chem. Soc*. **1997**, *119*, 12669.

(49) Schleyer, P. v. R.; Manoharan, M.; Wang, Z. X.; Kiran, B.; Jiao, H.; Puchta, R.; Hommes, N. J. R. v. E. *Org. Lett.* **2001**, *3*, 2465.

(50) Dewar, M. J. S.; Ford, G. P.; Mckee, M. L.; Rzepa, H. S.; Thiel, W.; Yamaguchi, Y. *J. Mol. Struct.* **1978**, *43*, 135.

(51) Iwasa, Y.; Furudate, T.; Fukawa, T.; Ozaki, T.; Mitani, T.; Yagi, T.; Arima, T. *Appl. Phys. A* **1997**, *64*, 251.